THE PENNSYLVANIA STATE UNIVERSITY
SCHREYER HONORS COLLEGE

DEPARTMENT OF ENGINEERING SCIENCE AND MECHANICS

EVALUATION OF THE CRITERIA FOR CRACK PROPAGATION IN THE PRESENCE OF HIGH SURFACE STRESSES

KATELYN J. SMITH

Spring 2010

A thesis
submitted in partial fulfillment
of the requirements
for a baccalaureate degree
in Engineering Science
with honors in Engineering Science

Reviewed and approved* by the following:

Albert E. Segall
Professor of Engineering Science and Mechanics
Thesis Supervisor

Christine B. Masters
Assistant Professor and Undergraduate Program
Coordinator of Engineering Science and Mechanics
Honors Adviser

Judith A. Todd
P. B. Breneman Department Head Chair
Professor, Department of Engineering Science and Mechanics

* Signatures are on file in the Schreyer Honors College and Engineering Science and Mechanics Office.

ABSTRACT

The petrochemical industry is largely dependent on the continuous operation of equipment to turn the maximum profit. Thus, there exists an intricate balance between the financial gains of the business and the structural integrity of the equipment. Numerous standards are therefore used to establish an appropriate degree of conservatism in the design process to ensure safe and reliable long-term operation.

The standard under evaluation in this thesis research is the API 579-1/ASME FFS-1. The present methods for determining critical crack dimensions in this standard compare a calculated stress intensity value from the surface and depth locations with the material fracture toughness. In cases where high, residual stresses exist on the surface, this treatment may result in an overly conservative estimation of the likelihood of crack propagation due to the rapidly diminishing stresses as the crack face moves away from any high surface stresses. Since over-conservatism can be problematic, the goal of this project is to evaluate the critical crack assessment in the presence of a stress field that diminishes rapidly in the through-thickness direction.

Through the use of finite element analysis and other analytical tools, the depth and surface locations of a semi-elliptical surface crack were examined in terms of stress intensity solutions. A comparison between the standard and the finite element analysis confirmed that the critical crack-like flaw assessment provides an additional degree of conservatism at the depth location of the flaw; this inherent conservatism is equivalent to a safety factor of approximately 1.375 or higher for the cases reviewed. The surface location was unable to be properly assessed due to inconsistencies in the mesh applied at this location. Thus, further modeling work is necessary to accurately evaluate the level of conservatism at the surface location of the semi-elliptical crack.

TABLE OF CONTENTS

LIST OF FIGURES

LIST OF TABLES

ACKNOWLEDGEMENTS

First of all, I would like to thank my thesis adviser Dr. Albert Segall for supporting me throughout the course of my research and education. I have benefited from his guidance about the finer points of mathematics and mechanics. I am also grateful for his patience and ability to keep me focused on my research. I would also like thank those at The Equity Engineering Group who supported me in my research and my growth as an engineer. Specifically, I would like to thank David Osage and Ryan Jones for their assistance and support. To Warren Brown, I owe a great debt to his help with modeling and numerous facets of this thesis research. Lastly, I would like to offer a special thanks to Jeannie Lewis for her constant guidance and friendship; she was always willing lend a hand to support my work.

Chapter 1

Introduction

Petrochemical plants and oil refineries are vital to the operation of many industries across the United States. In fact, their operation is critical for the very maintenance of our industrialized civilization. As this industry is characterized by an aging infrastructure, it is important to adhere to procedures designed to both keep the working environment safe and the equipment operating at top capacity; the production loss from any downtime can be very high indeed. To illustrate the ramifications of unexpected shutdown, chemical plants have production loses ranging from $5000 to $100,000 per hour during these periods. Refineries can even experience production losses reaching millions of dollars [1]. Therefore, in order for a plant to operate cost-effectively, it must be running virtually uninterrupted with little or no constraints on performance [2]. These strict parameters reveal the importance of a failure-free operation.

1.1 Equipment Evaluation

Standards have been developed all over the globe to provide accurate assessments of the equipment in this industry; of these standards, API 579-1/ASME FFS-1 is the most widely practiced in the United States. While these codes are designed to preserve the structural integrity of the plant's equipment lifecycle, there also remains the major business objective of maximizing plant production levels. Hence, there exists a thin line between the interests of safety and production. An ideal standard reduces costs of downtime while ensuring that the proper precautions are taken to avoid failure; since equipment failure results in negative repercussions

not only for the business and the safety of the workers, but for the general public and environment as well.

Common assessment practices target degradation mechanisms such as corrosion, creep, fatigue, pitting, embrittlement, mechanical distortion, and hydrogen attack to evaluate the remaining strength of the component. One of the most useful practices requires the assessment of crack-like flaw. These flaws are very common in the petrochemical industry, (welds for instance), and can quickly grow to be dangerous. Given its importance, this research focused on such cracks by taking a further look into the workings and level of conservatism of the API 579-1/ASME FFS-1 standard.

1.2 Objectives

The present methods for determining critical crack dimensions in the API 579-1/ASME FFS-1 standard compare a calculated stress intensity value from a through-thickness stress distribution at the surface location with the material fracture toughness. In cases where high stress gradients exist such as in residual stress fields, this treatment may result in an overly conservative estimation of the likelihood of crack propagation.

As such, the goal of this research was to evaluate the accuracy of API 579-1/ASME FFS-1 through finite element analysis methods; this research assessed the level of conservatism when calculating acceptable critical crack dimension in the presence of a stress field that diminishes rapidly in the through-thickness direction. All work described herein is actually the first step in the overall goal to determine an improved criteria for crack propagation in the presence of high surface stress and was conducted on behalf of The Equity Engineering Group.

Chapter 2

Background

A discussion of some basics is necessary in order to fully understand the scope of the problem and the methods of evaluation. This thesis begins by presenting the literature concerning stresses and their relation to pressure vessels (2.1), followed by a further look into determining critical crack dimensions in the API 579-1 /ASME FFS-1 calculate (2.2), and an inspection of the role of the weight function (2.3).

2.1 Pressure Vessel Stress Assessment

The design code targeted in this work is a common United States standard for the assessment of crack-like flaws for the refinery and petrochemical industry; thus the main structures evaluated are pressure vessels, tanks, and piping. Pressure vessels are sealed containers designed to hold contents at a pressure varying greatly from the ambient. These structures, which experience extreme temperatures, pressures, and environments, must be designed carefully to avoid failure, extensive property damage, and physical injury that can follow.

2.1.1 Characterization of Stress

Stress, the measurement of force per unit area, is a tensor quality; thus, it is dependent on both the direction of the applied load in addition to the plane it acts on. Most planes contain both normal and shear stresses. However, there exist planes known as principal planes with only

normal stresses acting on them. Since the magnitudes are large, these principal stresses play an important role in the design process.

Stress can generally be categorized into primary or secondary values; these are denoted by P or Q respectively according to the ASME (American Society of Mechanical Engineers) Boiler and Pressure Vessel Code [3]. Primary stresses are normal or shear stresses directly resulting from the loading conditions, and are needed to fulfill the equilibrium parameters of the vessel. Primary stresses typically result from mechanical loading, such as pressure and can result in failure if they exceed the ultimate stress. Given their complex nature, primary stresses are often further broken down into primary membrane and bending stresses; the membrane stress is distributed across a solid section and the bending stress is the linearly varying component proportional to the distance from the centroid of the solid section. In contrast, secondary stresses generally arise from stress concentrations or geometric discontinuities [4]. Such stresses satisfy strain or displacement conditions rather than the equilibrium of the structure. Since they often arise from mechanical or thermal loads, the secondary values must always be paired with a primary stress.

Other significant stresses are those that remain after the original load, or cause of stress is removed. Residual stresses can occur for a variety of reasons including, but not limited to, heat treatment and inelastic deformation. Furthermore, welding is a process that often generates residual stresses due to the heating and cooling of the weld metal and neighboring heat affected zones [5]. Lately, as residual stresses are becoming more widely understood, it has also become apparent that a more reliable method is needed to describe them in order to meet current assessment requirements [6]. In fact, it is important to be able to accurately model the residual stress distributions since they can have a significant impact on failure behavior. Residual stresses

are very important in the vicinity of cracks or notches since they can influence the promotion or inhibition of crack growth by their respective tensile or compressive qualities [7].

2.1.2 Origin of Stresses in Pressure Vessels

Most failures in pressure vessels stem from the presence of high stresses. For this reason, it is critical to accurately obtain any stress distributions in the vessel as well as identify their impact on the structural integrity. Mechanical loads such as weight, pressure, and environmental factors are often responsible for the stresses in the vessel. Additionally, as already mentioned, it is important to consider the implications of residual stresses that may arise from manufacturing or other conditions.

2.1.3 Stress Intensity Factor

A stress intensity factor is a parameter commonly used in fracture mechanics and is often represented by "K." This generalized construct embodies the effects of structural geometry, crack dimensions, and the distribution of the stress field [8]. Stress intensity factors can be categorized into Mode I, II, and III to reflect how the crack is opened. Mode I is the most commonly occurring of the three [9] as it is the tensile or opening mode where the surfaces of the crack move directly apart. As the stress intensity factor represents the intensification of the stress at the crack tip, the fracture toughness, K_c is the highest allowable magnitude of the stress intensity. Thus, if the value of the stress intensity exceeds the fracture toughness, unstable crack growth and fracture will occur. In general, fracture toughness is a measure of the stress level necessary to

propagate a preexisting flaw. This preexisting flaw may emerge as a crack, weld defect, metallurgical inclusion, void, design discontinuity, or some mixture thereof [9].

The research described in this thesis is focused soley on surface cracks, either internal or external. External cracks can form from a host of different causes including environmental corrosion, support welds, and preexisting flaws. Likewise, internal cracks can often result from similar reasons including hydrogen corrosion and pressure effects. Regardless of the origin and positioning of the crack, surface cracks are treated as a semi-elliptical geometry because Lin and Smith[10] found that a crack with any arbitrary intitial shape will eventually grow into, and propogate as a semi-elliptical shape in pressure vessels. Consequently, this research focused on the modeling of semi-elliptical geometries as pictured in Figure **2-1**.

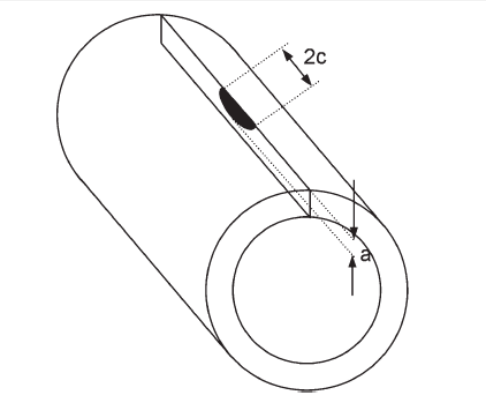

Figure 2-1: *A three-dimensional semi-elliptical external crack* [11]. Axial cracks may occur on either the external or internal surfaces and can be oriented in the axial, circumferential, or inclined directions.

To summarize, the current modeling assumptions indicate that the choice of a semi-elliptical surface crack is appropriate. One more simplification was used in order to create a simplified geometry and mesh situations. This simplification was the use of a flat plate as the crack modeling surface, as shown in Figure **2-2**, rather than a cylindrical or spherical structure; such an approximation can be utilized with the introduction of a surface correction or bulging factor [12]. Accordingly, stress intensity factors solutions for a flat plate with a surface semi-elliptical flaw were used.

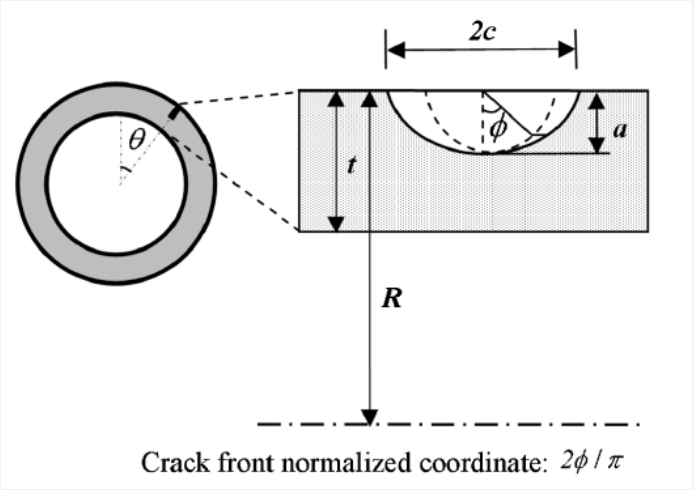

Figure 2-2: *Geometry with an external axial crack of semi-elliptical shape* [11]. For this evaluation, a flat plate will be used to model all crack-like-flaws.

2.2 API 579-1 /ASME FFS-1 Standard

The API (American Petroleum Institute) and ASME design codes provide rules for the design, fabrication, testing, and inspection of pressurized equipment [13]; as such, the API 579-1/ASME FFS-1 is the standard evaluated in this work. Fitness-For-Service (FFS) evaluations are qualitative assessments of in-service equipment that may contain damage of some form

compromising the structural integrity. This assessment is required for a number of reasons including the following: "maintaining the safety of plant personnel and the public, complying with OSHA 1910 process safety management (PSM) rules, protecting the environment for accidental releases of damaging substances, reliably operating aging facilities, maintaining safe and reliable operations with increased run lengths and decreased shutdown periods, determining the feasibility of increasing the severity of operations, rationalizing the damage found by more rigorous in-service inspections than found by inspections performed during original construction [14]."Given these reasons, the publication was created as a "recommended practice" to replace previous conservative standards with a more sophisticated evaluation of metallurgical conditions and analysis of local strains and stresses [15].

2.2.1 Background of the API 579-1 /ASME FFS-1 Standard

In January 2000, the American Petroleum Institute published the Recommended Practice 579 Fitness-For-Service to present the petroleum industry with a sound guide to use in the evaluation of the structural integrity of equipment [13]. As envisioned, this standard was to be used in conjunction with existing codes such as API 510, API 570, and API 653 to produce reliable assessments to ensure the safety of workers and the public while also optimizing equipment performance. Each code was constructed by a committee consisting of the API, Chemical Manufacturers Association, and industry professionals to incorporate the best Fitness-For-Service methods. ASME, while concurrently developing a parallel standard, joined API in a collaboration to create the standard in 2001. Due to the ever-present need for continuous refinement and advancement in the engineering field, the American National Standards Institute approved the updated version of this standard in 2007 as API 579-1/ASME FFS-1 [13]; this standard is currently the most commonly used across the United States for the industry.

2.2.2 Critical Crack Calculation in the API 579-1 /ASME FFS-1 Standard

The API 579-1/ASME FFS-1 under evaluation in this research is a highly structured system which is organized by damage mechanism. A consistent Fitness-For-Service methodology for damage assessment is followed throughout each section to promote ease of use. An assessment procedure for evaluating crack-like flaws is presented in section nine of this standard. While there are many important aspects, the Failure Assessment Diagram (FAD) forms the basis of the flaw evaluation in this section [16]. A FAD diagram is a two-parameter approach to assessing a flaw. A point plotted below the FAD curve is acceptable; whereas, any point above the FAD curve is unacceptable and the flaw must be reassessed. This diagram also accounts for unstable fracture and plastic collapse separately as shown in Figure **2-3**. Furthermore, it should be noted that this method is the recommended practice for other prominent procedures such as R6 and BS 7910 [13].

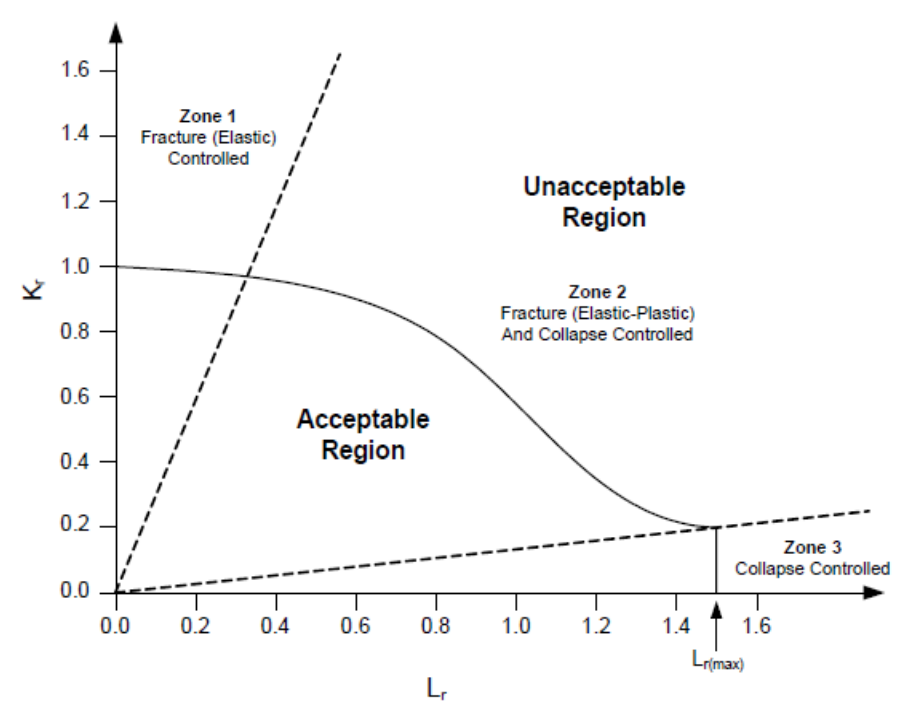

Figure 2-3: *Failure Regions on the Failure Assessment Diagram* [17].

The FAD diagram can be divided into three zones to predict failure by the placement of a calculated point. Zone 1 is connected with brittle fracture while Zone 3 is coupled with immense yielding from large deformation. Hence, if the point lies in Zone 2, then the predicted method of failure is elastic-plastic fracture. Essentially, the FAD compares the load ratio, or the reference stress over the lower yield stress and the fracture ratio, or the applied stress intensity factor over the material fracture toughness. The load ratio can be described in terms of the crack-tip plasticity, whereas, the fracture ratio is represented by the elastic driving force. Essentially, a flaw is considered stable and thus acceptable, if its representative point lies within the FAD curve.

The first step in the assessment completed in this thesis was to evaluate the applicability and limitations of the specific parameters. Constraints on factors such as material use, loading conditions, and flaw characterization allow for the classification of the assessment into one of three levels. Each level is constructed to have a balance between conservatism and the quantity of information needed. With this in mind, Level 1 will be the most basic and can be utilized with the least amount of inspection, while Level 3 has the most detailed evaluation [9].

The second step towards constructing the FAD diagram is to gather the necessary data for calculations. Data requirements will be specific to the damage mechanism and level; however, most procedures require original design information, maintenance and operating history, and flaw data. One vital component of this data is the classification and quantification of the stresses acting on the flaw. Stresses are derived from the future loading conditions and are also based on the uncracked geometry at the flaw location [16]. However, stress distributions can vary across the surface of the flaw and through-thickness. For the purpose of narrowing the focus of this research, only distributions varying through the thickness were examined for their influences on the conservatism of the calculation.

If the only loading acting on the structure is pressure producing a membrane stress field, then a Level 1 calculation can be used to determine the stress field. However, if bending and supplemental loadings are present, then a Level 2 or Level 3 assessment must be employed. Both Levels 2 and 3 have the same parameters for assessing stresses and thus stress intensity factors; these Levels simply differ on their construction of the FAD diagram. A Level 2 or Level 3 assessment may then be used to fulfill the stress evaluation in conditions when complicated geometries or loading conditions call for advanced stress analysis techniques, or there are high gradients in the stress field [16].

As already mentioned, this research took a closer look at the use of a Level 2 assessment because it is the most basic evaluation that still enables the incorporation of stress fields varying in complexity and exhibiting a high stress gradient at the surface location. Level 2 classifies stresses as primary, secondary, or residual and then calls for the computation of the reference stresses based on the distributions of each using the solutions in Annex D. Once the reference solutions are obtained, they can be used to calculate the stress intensity factors for both primary stresses as well as secondary combined with residual stresses by use of Annex C [16].

The API 579-1/ASME FFS-1 offers stress intensity factor solutions for several different stress profiles. These stress profiles are first categorized as either a linear, fourth-order polynomial, or arbitrary stress distributions. Since the solution using an arbitrary stress field can accurately compute highly non-linear and varied stress profiles, this method will be used for the stress intensity factor calculations. Through this method, any stress distribution can be used to directly determine a stress intensity factor by integration with a suitable weight function; the weight function approach presented in Equation **2-1** is used in this assessment. In Equation **2-1** the parameter $h(x,a)$ is the weight function and $\sigma(x)$ is the stress normal to the flaw with the variable x representing the distance through the thickness of the plate. In addition, f_w is the finite

width correction factor and a is the crack depth. The following equation calculates K_I or the Mode I stress intensity factor [12]:

$$K_I = \left[\int_0^a h(x,a)\sigma(x)dx \right] f_w \qquad 2.1$$

Equation 2.1 is used for calculations at both the surface-breaking location of the semi-elliptical crack and at the depth location along the crack front, also known as the zero and ninety degree locations, respectively [12]. According to Level 2, the stress intensity factors are calculated separately for primary stresses as well as secondary and residual stresses. Also, it is important to note that stress intensity factors are equated to zero if they have a negative value; thus, compressive stresses are not factored into the calculations. This is a conservative measure in the standard because the normal nature of compressive stresses is to suppress the growth of the crack.

The next step in the critical crack growth evaluation is to calculate the plasticity interaction factor. When both primary and secondary or residual stresses are applied, the plasticity interaction factor is evaluated through the use several tables to compute the load ratios of the secondary and residual stresses. If this ratio is greater than four, then the stress intensity factor corrected for plasticity effects must be computed; an alternative simplified model is also offered to pass through this step. In addition, the process is simplified if only one type of stress is found; any correction factors are applied to this value that is then divided by the materials fracture toughness to find the toughness ratio. It is important to note that these stress intensity factors directly impact the magnitude of the toughness ratio calculation.

With the completion of the calculations just discussed, it is time to turn to the FAD diagram for the final appraisal. A point can be plotted on the FAD diagram from the determined coordinates of the toughness and load ratios; the load ratio is the reference stress divided by the

yield strength. Once again, if the assessment point lies inside the curve, then the crack is considered safe; if the assessment point lies outside the curve, the crack may experience unstable growth. These calculation procedures can be observed in Figure **2-4**.

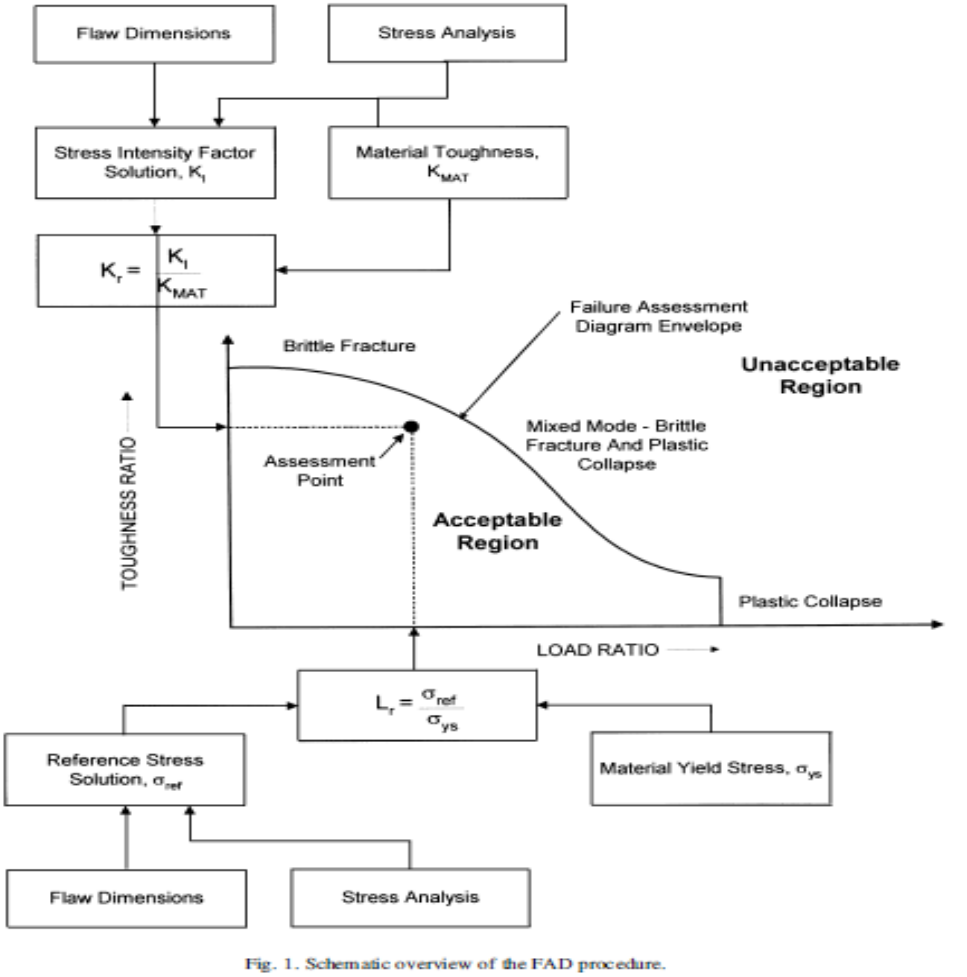

Figure 2-4: *Schematic Overview of the FAD Procedure* [13]. The above schematic illustrates the relationships between various calculations that form the FAD. It is shown that the stress analysis procedures, and thus the varied stress distributions, directly impact the reference stress solutions and the stress intensity factor solutions.

2.3 Weight Function Application

A weight function is a mathematical tool used during calculations to give some elements additional "weight," or influence on the solution than other elements in the same set. Since weight functions have been proven to efficiently calculate stress intensity factors for a variety of boundary conditions and under different loading scenarios [18], this method is used in the API 579-1/ASME FFS-1 standard for the assessment of stress intensity factors under arbitrary through-thickness loading conditions. Semi-elliptical cracks complicate assessments because in most cases they have to be calculated in three dimensional bodies [19]; fortunately, the weight function method can be applied to overcome any complex three dimensional calculations.

For evaluation purposes, API 579-1/ASME FFS-1 was compared to a weight function method for surface semi-elliptical cracks developed by Niu and Glinka [19]. The weight functions were constructed from the derivations of the Bueckner-Rice definition of weight function [19]:

$$m(x,a) = \frac{H}{K_r} \cdot \frac{\partial u_r}{\partial a} \qquad 2.2$$

The Bueckner-Rice equation is a weight function for a two-dimensional, cracked body under Mode I loading. The crack opening displacement field u_r is a function of the crack depth and the through-thickness distance. This equation relies on the ability to obtain a reference stress intensity factor K_r for the particular geometry and the stress system S_r. Additionally, the generalized modulus of elasticity is represented by H.

The Niu and Glinka weight function was also construction from the Petroski-Achenbach crack opening displacement expression [19]:

$$u_r(x,a) = \frac{\sigma_0}{H\sqrt{2}}\left[4F\sqrt{a(a-x)} + \frac{G(a-x)^{3/2}}{\sqrt{a}}\right] \quad 2.3$$

where $$F = K_r/\sigma_0\sqrt{\pi a} \quad 2.4$$

The Petroski-Alchenbach requires knowledge of the reference stress intensity factor K_r, a generalized modulus of elasticity H, and the characteristic stress σ_o. The parameter G is given as the following [19]:

$$G = \frac{(I_1 - 4F\sqrt{a}I_2)\sqrt{a}}{I_3} \quad 2.5$$

Where the definitions of I_1, I_2, and I_3 are given by:

$$I_1 = \sigma_0\pi\sqrt{2}\int_0^a F^2 a \, da \quad 2.6$$

$$I_2 = \int_0^a \sigma_r(x)(a-x)^{1/2}\,dx \quad 2.7$$

$$I_3 = \int_0^a \sigma_r(x)(a-x)^{3/2}\,dx. \quad 2.8$$

Additionally, the distribution of local reference stresses normal to the prospective crack plane ,σ_r is given by the following [19]:

$$\sigma_r(x) = \sigma_0 p(x) \qquad 2.9$$

In Equation 2.9, p(x) represents the normalized stress distribution with respect to the characteristic stress σ_o.

The weight function developed by Niu and Glinka assumes that the one-dimensional displacement function of Petroski-Achenbach can also be applied for semi-elliptical surface-cracks in flat plates. Niu and Glinka worked towards developing a closed-form solution for the weight function contained in a finite thickness plate. Their results were then validated by a comparison to the finite element data of Newman and Raju and Isida [20]; Newman and Raju produced the most widely used stress intensity factor solutions for cracks under pure bending and tension.

Chapter 3

Modeling

Finite element analysis (FEA) methods were used in this thesis research to evaluate the API 579-1/ASME FFS-1 2007 standard. ABAQUS/CAE is the software used for modeling and FEA purposes; this software is a commercial package marketed under the SIMULIA brand of Dassault Systemes. ABAQUS/CAE is a tool used to efficiently create models, perform analysis, and view results, and the computer-aided engineering capabilities allow the user to explore real-world behavior. In addition, ABAQUS/CAE is not limited to the petrochemical and refinery industries; this software has numerous applications in the aerospace, automotive, and industrial product industries as well.

3.1 Finite Element Analysis

Finite element analysis, also referred to as the finite element method, is a numerical procedure used to find approximate solutions to integral equations and partial differential equations. This methodology simplifies complex continuum problems by approaching them in a series of smaller interrelated simple problems. In FEA, mathematical physics applications are solved through the approximations of geometry and the response variables or fields of the problem [21].

Today, finite element analysis is a powerful computer-based tool widely used throughout engineering and science disciplines. Modern computers are capable of performing the computational tasks necessary to use this methodology. Evolution of computers is in part responsible for generating the many advancements pertaining to the study of FEA since its

introduction in the early 1960s. The overall production cycle including design, development, testing, and analysis has been greatly accelerated with this tool. Additional benefits of current FEA methods include improved accuracy, enhanced knowledge of critical design parameters, virtual prototyping, and reduced simulation costs.

FEA configures a model by assembling a system of points or nodes which all together form a structure known as a mesh. This mesh has defined properties from structural characteristics and material properties. The nodes are configured into a particular form and density across the geometry; these are dependent on the stresses applied across precise areas. Generally, areas anticipating elevated or rapidly changing stress distributions are characterized by a higher nodal density than the areas with little or no stress.

3.2 Model Design

As previously discussed, the design for this research consisted of a flat plate with a semielliptical, surface flaw. The process of creating a FEA model involves many variables, and each variable is capable of greatly impacting the final output. Therefore, specific constraints were implemented in order to create a design that represented a common field case in the industry.

The first step in this design process was to determine the necessary geometry and construct the physical components. The flat plate was constructed with a basic 10 x 10 x 1 inch geometry, and a common crack design was built into the plate with the dimensions provided in Table **3-1**. Although these dimensions were arbitrary, the geometries were each compatible with the two weight functions used for comparison in this research. In order to apply the API 579-1/ASME FFS-1standard, the following dimensional limits must be satisfied [12]:

Crack and geometry dimensional limits:

1) $0.0 < a/t \le 0.8 \quad for \quad 0.0 < a/c \le 0.2$
2) $0.0 < a/t \le 1.0 \quad for \quad 0.2 < a/c \le 2.0$
3) $0.0 < a/c \le 2.0$
4) $0.0 < c/W < 1.0$
5) $0 \le \varphi \le \pi$

3.1

In addition, the following parameters must be met in order to apply the Niu and Glinka weight function for a surface semi-elliptical crack in a finite thickness plate:

$$K = \sigma_0 \sqrt{\pi a} F\left(\frac{a}{t}, \frac{a}{c}, \frac{c}{w}, \phi\right)$$

for $a/t < 1.25(a/c + 0.6)$ and $0 \leqslant a/c \leqslant 0.2$

or $a/t < 1$ and $0.2 \leqslant a/c \leqslant \infty$

3.2

The requirements given in equations 3.1 and 3.2 were satisfied by the dimensions of the model construction.

Table 3-1: *Dimensions of ABAQUS/CAE Model for Semi-elliptical Crack Growth*

Model Dimensions (in.)	
Plate Thickness (t)	1.00
Plate Width (w)	10.00
Plate Length (l)	10.00
Crack Depth (a)	0.20
Crack Length (2c)	2.845
Ratio of a/c	0.14058
Ratio of a/t	0.2000
Ratio of c/l	0.14225

3.2.1 Crack Construction

When simulating a flaw in three dimensions, a seam crack is modeled as a face partition entirely embedded into the solid body; this task can be performed by partitioning or using a cut operation. Partitioning the model is particularly important because a single layer of wedge elements must be created along the crack-front. After all of the partitions are created for meshing purposes, the original definition of the seam remains intact. All edges must be seeded properly to create a focused mesh around the crack front while maintaining minimal mesh distortion throughout the component.

One important aspect of modeling a crack in ABAQUS/CAE is defining the direction of crack extension. In three dimensional applications of semielliptical flaws, the proper practice is to apply q vectors in the virtual crack extension direction. These vectors must be individually adjusted by selecting nodes defining the direction normal to the crack seam. The process of adjusting q vectors should start at the depth location and define the crack line sequentially till the other end of the contour is reached.

In the modeling of the semi-elliptical crack, a contour integral evaluation was used to obtain the stress intensity factors. Each contour is a ring of elements fully surrounding the crack tip, or the nodes along the crack line, from one starting crack face to the opposite ending crack face. The first contour consists of the crack front and one layer of elements surrounding it, and the second contour then consists of the ring of elements touching the second contour as well as the original first contour. Accordingly, each successive contour is characterized by the elements contacting the previous contour as well as that contour itself. Each contour allows for an evaluation at that node; therefore, the number of evaluations is dependent on the number of rings present. Overall, a semielliptical flaw was constructed by drawing the crack seam, specifying propagation directions, and modeling the contours surrounding the seam.

An additional consideration when creating a FEA model is characterizing the crack tip. When defining a 3-dimensional complex model, it is difficult to obtain the fracture parameters around the crack tip due to the complication of stress distribution at this locality. In mathematical calculations, stress experiences a singularity at this location and approximations perform poorly. In order to combat this singularity at the crack tip, a singular element is used at this point [22].

3.2.2 Loading Specifications

One of the main tasks of designing a model is to accurately represent the desired loading or boundary conditions. In this research, the aim was to reproduce a residual stress field characterized by a high magnitude at the surface of the plate and rapidly decreasing through the thickness until a compressive zone was reached. Boundary conditions were implemented through the application of an initial load producing the desired residual stresses; this loading was applied perpendicular to the thickness through a user constructed subroutine. Two loading scenarios, varying in magnitude were applied to create separate solutions for evaluation. The loading profile with the higher magnitude was labeled as “Load 1,” and the loading profile with the lower magnitude was referred to as “Load 2.”

3.2.3 Material Selection

Material selection is an important step in most design processes. In order to construct a model representing common designs found in the refinery and petrochemical industries, SA 516 was used. This material is commonly used in both industries and is particularly abundant in the construction of pressure vessels. Since there are several grades of this steel, the most regularly

found SA 516 grade 70 was applied to the model. Elastic properties for this material include a modulus of elasticity of E= 29 x 10^6 psi and a poison's ratio of ν= 0.3; these parameters were specified in the model with the assumption that the structure will not be experiencing any extreme temperatures where E and ν could vary.

3.2.4 Additional Model Construction Parameters

Several factors must be addressed in addition to crack geometry, loading specifications, and material selection when constructing a model in ABAQUS/CAE. As already discussed, one such factor is the application of boundary conditions to allow for loads to behave as expected. Three boundary conditions are illustrated by the cut-away view in Figure **3-1.** The model has a symmetry condition for the y variables illustrated by the blue boundary plane. Additionally, the flat plate is bounded by displacement and rotation restraints in the z and y-directions as shown by the orange boundary planes. These three conditions permit the through-thickness loading to operate effectively without displacement or rotation of the modeled plate.

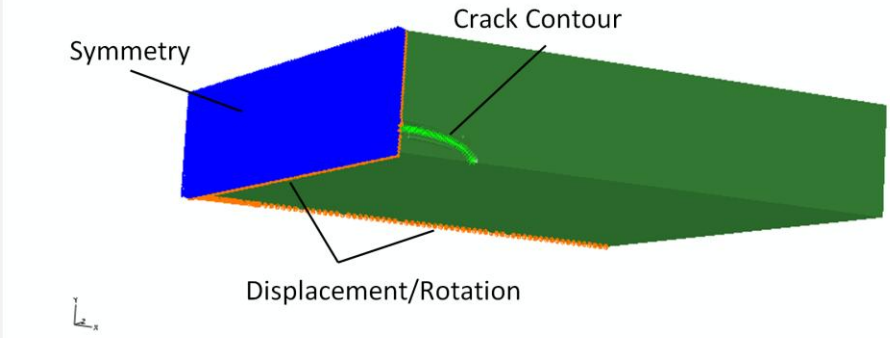

Figure 3-1: *Cut-Away View of Modeled Crack and Boundary Conditions.* The above figure shows a cut-away quarter view of the flat plate model with boundary conditions applied.

Chapter 4

Results

As discussed, the critical crack assessment is directly determined by the comparison between stress intensity factors and the fracture toughness of the material. Stress intensity factors were obtained from the contour integrals around the seam of the modeled semielliptical crack. Results from the ABAQUS/CAE model were then compared to the analytical results of the API 579-1/ASME FFS-1 standard. Furthermore, these values were compared to the Niu and Glinka weight function for semi-elliptical surface cracks as an additional reference. The aim in this analysis was to observe if the API 579-1/ASME FFS-1 standard produces conservative results compared to the ABAQUS/CAE model and if so, to quantify the degree of conservatism.

4.1 Finite Element Analysis Results

The stress intensity factors in this research were gathered from the inspection of the fifth contour surrounding the crack seam. In ABAQUS/CAE, values are typically based on the average of contours three to five in each mesh. Generally, a larger contour produces a more accurate stress intensity value. These stress intensity factors are of course dependent on the ability to apply an appropriate mesh to the model. The results for the ABAQUS/CAE model are provided in Table **4-1** for each load and respective location.

Table 4-1: *Stress Intensity Values for ABAQUS/CAE Model*

ABAQUS/CAE MODEL RESULTS

Location of Stress Intensity Factor	Load 1 (psi$\sqrt{in}$)	Load 2 (psi$\sqrt{in}$)
Surface (0 degree location)	18900	15324
Depth (90 degree location)	32500	26506

Stress intensity factors are also dependent on the S33 Principal Stress which acts as a driving force for crack propagation. The stresses normal to the crack resulting from the loading conditions are illustrated in Figure **4-1** and Figure **4-2**. These images offer both a view of the whole model as well as a close-up of the crack after the loading has been applied; the highest stress values were observed at the depth location of the semielliptical crack.

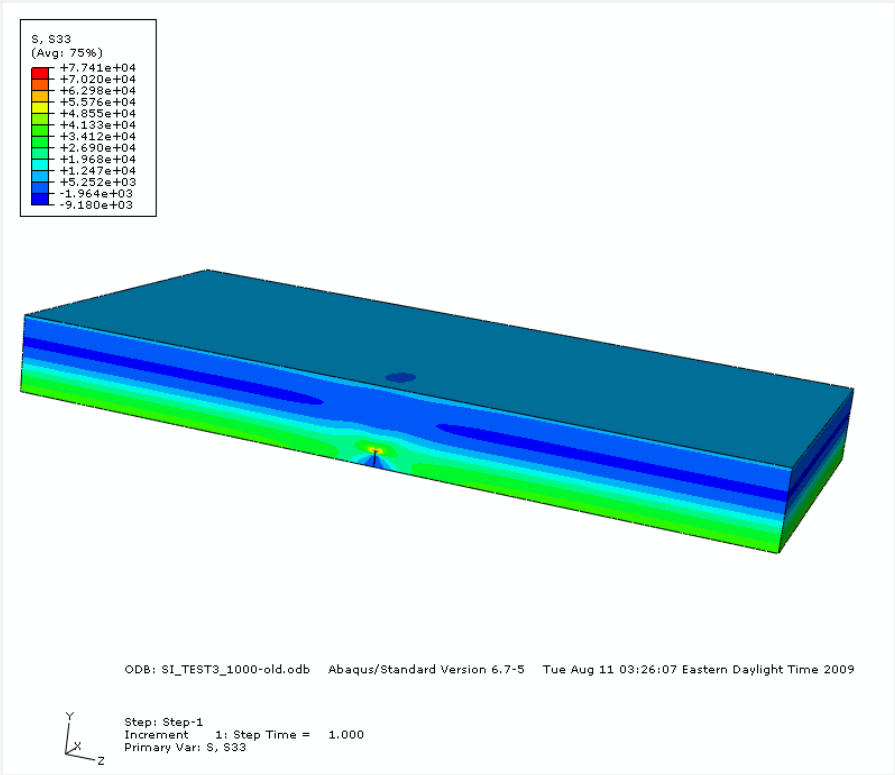

Figure 4-1: *View of Load 2 Undeformed Stressed State.* The above figure shows a view of the stressed state of the flat plate.

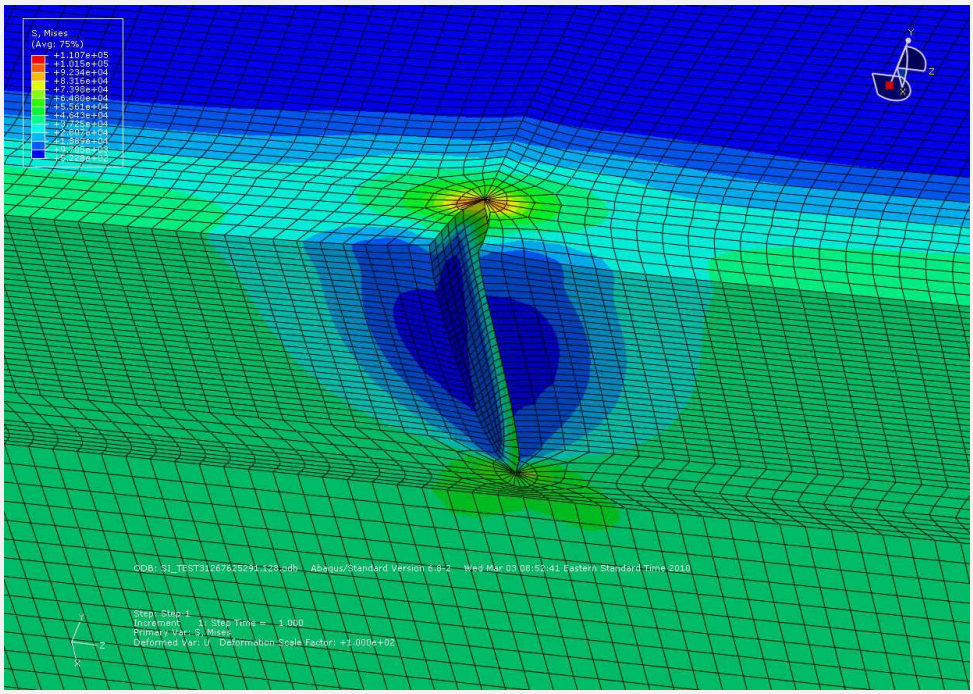

Figure 4-2: *View of Load 1Deformed Stressed State.* The above figure shows a close view of the stressed state of the flat plate with the crack opening.

The semielliptical geometry of the crack presented difficulties when meshing the model. While the mesh applied to the depth of the crack was constructed with a consistent geometry, it proved difficult to apply a consistent element structure to the surface location because the crack was relatively shallow. Since difficulties were experienced in the meshing procedure, the stress intensity results were not consistent at the last value at each end of the contour needed for evaluation. To combat this behavior, the stress intensity factors were approximated by a linear fit using the points exhibiting normal behavior in these areas, and these results are provided in Table **4-2**. A linear fit was used because the values had a general linear nature along the semielliptical crack contour. During this approximation method, the depth location behaved more consistently across the third, fourth, and fifth contours than the surface value. This consistent performance is reflected in the degree of precision shown in the approximation results for the fifth contour.

Table 4-2: *Linear Approximation of Stress Intensity Values for ABAQUS/CAE Model*

ABAQUS/CAE MODEL LINEAR APPROXIMATION

Location of Stress Intensity Factor	Load1 (psi$\sqrt{in}$)	Load 2 (psi$\sqrt{in}$)
Surface (0 degree location)	17000-18000	14000-15000
Depth (90 degree location)	~27600	~22400

4.2 Analytical Work

This section of the thesis includes the steps taken to calculate the stress intensity factors through the use of the API 579-1/ASME FFS-1 standard for the same conditions modeled in ABAQUS/CAE. Additionally, stress intensity solutions from the weight function produced by Niu and Glinka were used for a comparison to the weight function method in the API 579-1/ASME FFS-1 standard.

4.2.1 API 579-1/ ASME FFS-1 Analysis

The stress distributions through the thickness of the plate were calculated in order to move forward with the comparison of these three methods. Distributions of the stress through the thickness of the flat plate was retrieved from the two loading cases in the ABAQUS/CAE model and then fitted to polynomial functions. These distributions were calculated from a location on the plate removed from any geometric interference. Each function was representative of the loading applications, material selection, and boundary conditions as well as other constraints found in the model. The complete stress outputs for Load 1 and Load 2 are provided in Appendix A. In addition, Figure **4-2**and Figure **4-3** provide graphical representations of the through-

thickness stresses. Figure **4-5** and Figure **4-6** then offer a polynomial fit to the stress components driving the crack (also known as the S33 stress).

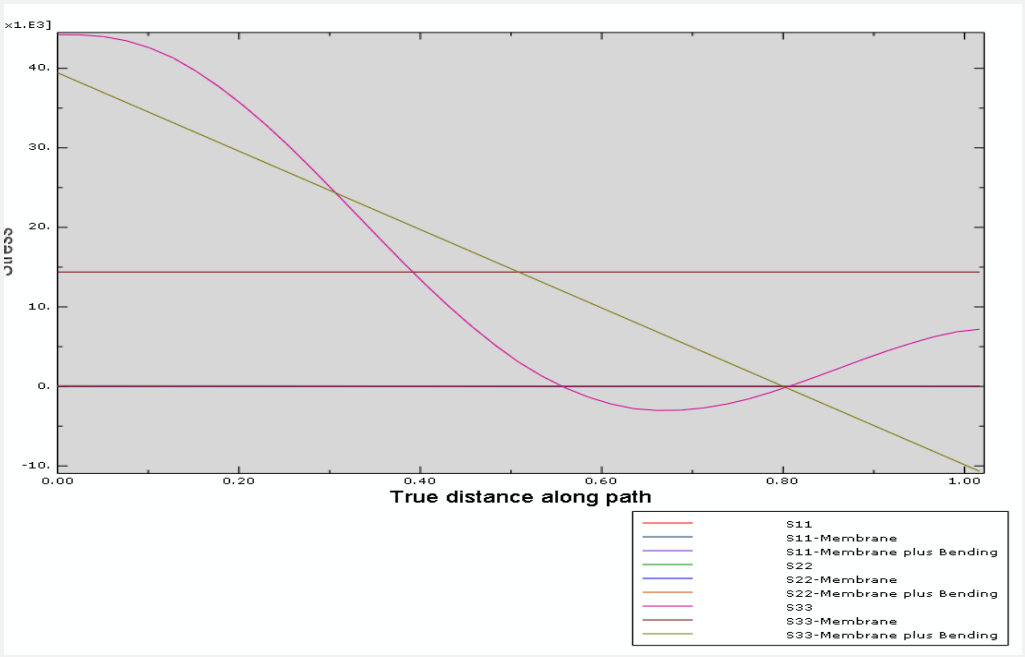

Figure 4-3: *ABAQUS/CAE Stress Linearization Through-Thickness for Load 1.* The figure above graphically displays the stresses on Load 1 representing a pre-crack state.

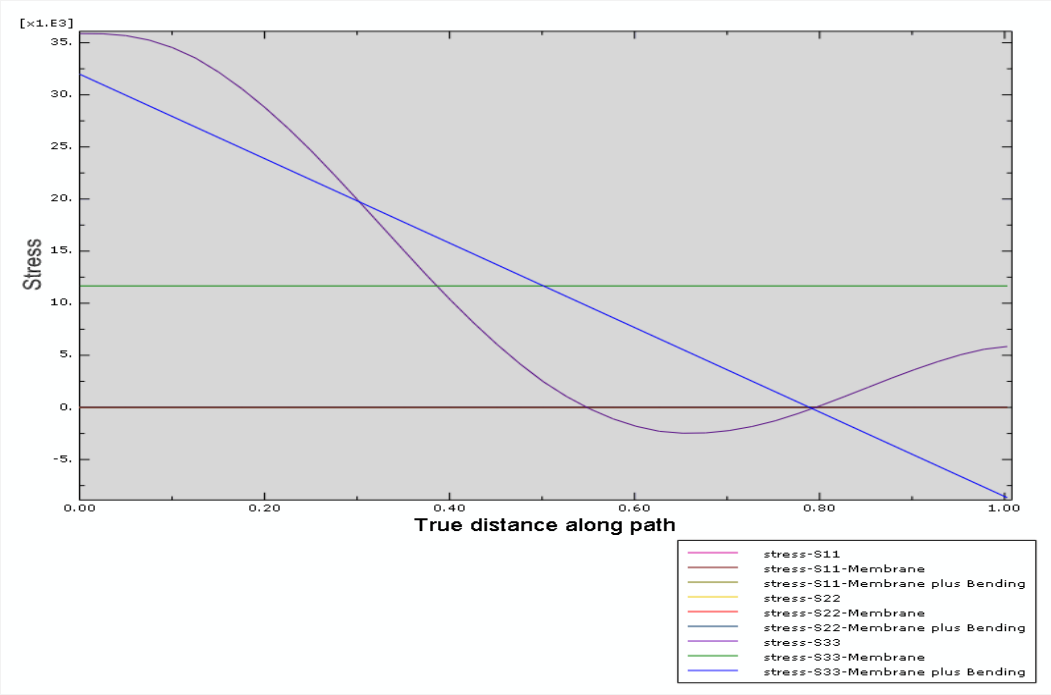

Figure 4-4: *ABAQUS/CAE Stress Linearization Through-Thickness for Load 2.* The figure above graphically displays the stresses on Load 2 representing a pre-crack state.

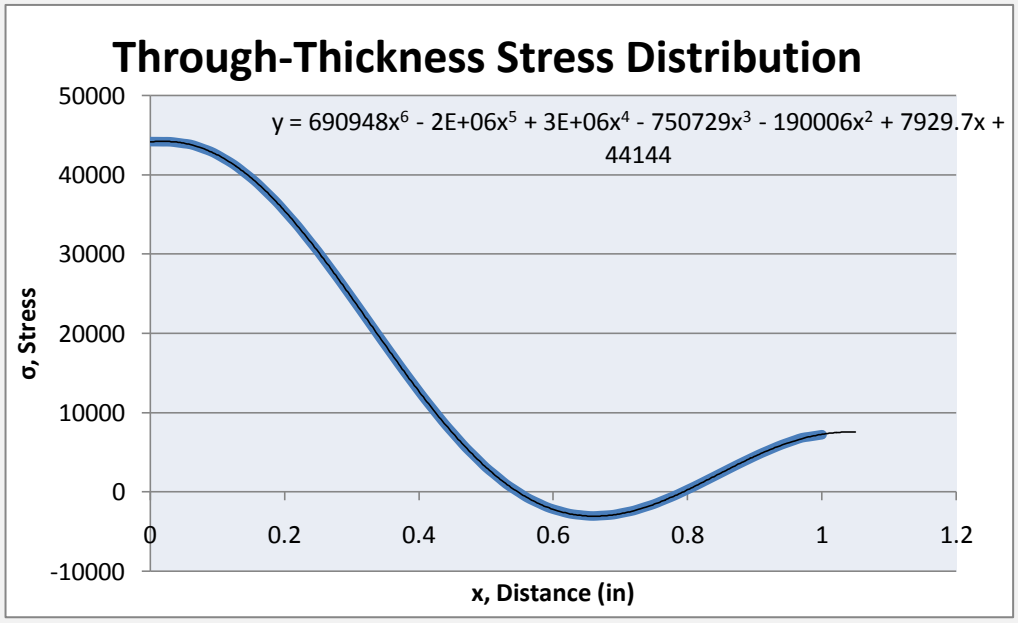

Figure 4-5: *Polynomial Fit to Stress Normal to Crack for Load 1* .The figure above shows the varying S-33 stress normal to the crack front and the polynomial equation that characterizes the stress curve.

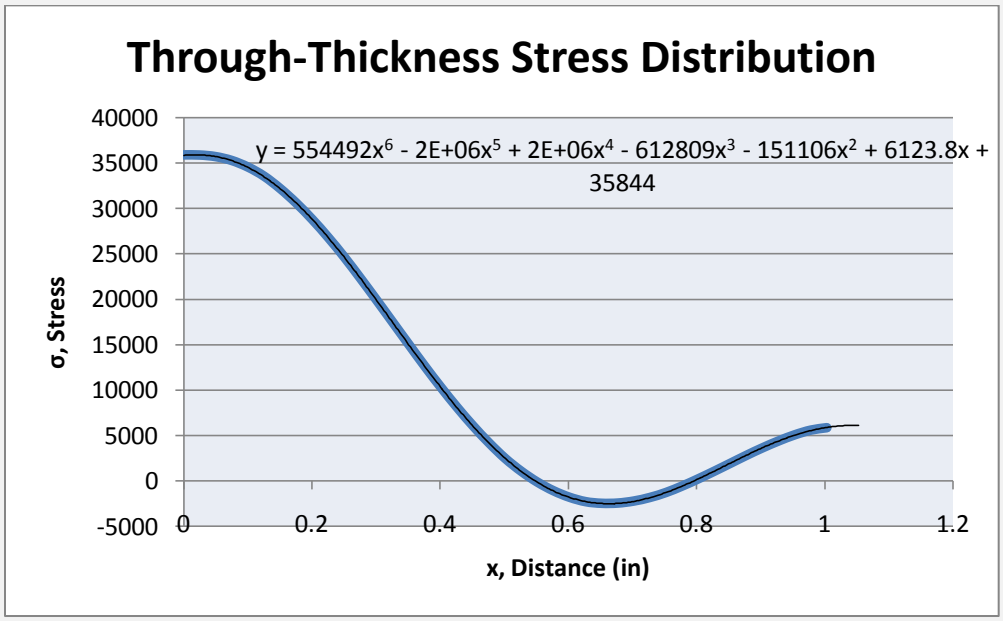

Figure 4-6: *Polynomial Fit to Stress Normal to Crack for Load 2* .The figure above shows the varying S-33 stress normal to the crack front and the polynomial equation that characterizes the stress curve.

The polynomial stress functions given in Figure **4-3** and Figure **4-4** were inserted into the API 579-1/ASME FFS-1 stress intensity factor calculation for a through-wall arbitrary stress; this was done to assure an identical stressed state was used for comparison. The code was evaluated for stress intensity factor values at the depth and surface locations of the crack through the use of Mathcad, an engineering calculation software produced by Parametric Technology Corporation. A Mathcad program was created from the weight function calculations given in the Annex C [12] of the standard and the computed stress distributions were easily imputed for each load. The Mathcad program is shown in Appendix B, and the results for API 579-1/ASME FFS-1are provided in Table **4-3**.

Table 4-3: *Stress Intensity Values from API 579-1/ASME FFS-1Standard*

API 579-1/ ASME FFS-1 RESULTS

Location of Stress Intensity Factor	Load 1 ($psi\sqrt{in}$)	Load 2 ($psi\sqrt{in}$)
Surface (0 degree location)	17350	14080
Depth (90 degree location)	38220	30810

4.2.2 Weight Function Comparison

The weight function for surface cracks in a finite thickness flat plate produced by Niu and Glinka was used as a comparison step to test if the stress intensity factor solutions obtained from the standard were analogous. This weight function was also programmed and evaluated via Mathcad. Similar to the method used to evaluate the standard, the same stress distributions were

inserted into this weight function program. Results are given for this evaluation in Table **4-4,** and the calculations steps can be found in Appendix B. In addition, a comparison between the three methods is given in Table **5-1**.

Table 4-4: *Stress Intensity Values from Niu and Glinka Work*

NIU & GLINKA STRESS INTENSITY FACTOR RESULTS

Location of Stress Intensity Factor	Load 1 (psi$\sqrt{in}$)	Load 2 (psi$\sqrt{in}$)
Surface (0 degree location)	15300	12260
Depth (90 degree location)	36800	29690

Chapter 5

Summary and Discussions

Through a comparison between the ABAQUS/CAE modeling, the API 579-1/ASME FFS-1 standard, and the weight function work of Niu and Glinka, the values at the crack depth exhibited the expected conservative behavior, while the values at the surface do not follow the same trend. A discussion of these results is presented in this section, and a comparison of these results is given in Table **5-1**. The two weight function approaches were compared against the finite element analysis method by percent difference calculations.

Table 5-1: *ABAQUS/CAE Comparison to Weight Function Methods*

	ABAQUS/CAE		API 579-1/ASME FFS-1		Niu and Glinka W.F.	
	Stress Intensity ($psi\sqrt{in}$)		Percent Difference (%)		Percent Difference (%)	
Load Name	1	2	1	2	1	2
Surface (0^o) Pt	17000-18000	14000-15000	(2.0)-(-3.7)	(0.6)-(-6.3)	(-10.5)-(-16.2)	(-13.3)-(-20.1)
Depth (90^o) Pt	27600	22400	32.3	31.6	28.6	28.0

5.1 Discussions

Since the behaviors of the two locations differ, the discussions of these locations were separated. The degree of conservatism at the depth location was assessed first, and a discussion of the results and complications at the surface location follows.

5.1.1 Depth Stress Intensity Factor

As presented in the results, the depth or ninety degree location returned stress intensity values of approximately 27600 psi$\sqrt{\text{in}}$ for ABAQUS/CAE Load 1 and 22400 psi$\sqrt{\text{in}}$ for ABAQUS/CAE Load 2. The results provided by the API 579-1/ASME FFS-1 standard were higher and thus more conservative than the ABAQUS/CAE results. The weight function developed by Niu and Glinka, which was projected to give similar solutions to those found by the standard, gave higher results for both loads as well. This was the case when the analytical methods were compared to both the given ABAQUS/CAE values and the linearly approximated values.

It was possible to approximate the factor of safety for the critical crack-life flaw calculation by measuring the solutions given by ABAQUS/CAE against the API 579-1/ASME FFS-1 standard results. The calculated safety factors for each load are provided in Table **5-2**.

Table 5-2: *Safety Factors from ABAQUS/CAE & Standard Comparison*

SAFETY FACTORS FROM ABAQUS/CAE & STANDARD

Load 1	Load 2
1.385	**1.375**

A partial safety factor is a quantity multiplied by the given value to achieve a target reliability level against the failure modes of fracture and plastic collapse in structural components.

Partial safety factors were not prescribed in the critical crack assessment steps. Any uncertainties in the numerous variables of the assessment were introduced in alternative locations of the standard through varying partial safety methods. For example, degrees of uncertainty may be incorporated into the calculation through the use of partial safety factors for flaw dimensions, fracture toughness, and stress application individually.

Given that safety factors were not incorporated into the assessment of critical crack-like flaws, the additional safety factor found in the calculation represents an additional degree of conservatism. Unfortunately, this conservatism is beyond the control of the user. In fact, anyone using this standard would normally be unaware of this additional level of conservatism in the critical crack assessment.

5.1.2 Surface Stress Intensity Factor

The surface or zero degree location returned stress intensity values of approximately 17000-18000 psi$\sqrt{\text{in}}$ for ABAQUS/CAE Load 1 and 14000-15000 psi$\sqrt{\text{in}}$ for ABAQUS/CAE Load 2. The results given by the API 579-1/ASME FFS-1 standard fell inside this range of values; however, this did not account for any additional degree of conservatism in the solutions. The weight function method created by Niu and Glinka gave values even lower than those provided by the standard. Thus, neither approach offered a conservative solution compared to the ABAQUS/CAE model results. Moreover, the ABAQUS/CAE solutions given by the two loads without the linear approximation method were above this calculated range.

After comparing the results at the surface, it is important to discuss why this location did not behave in a manner similar to the depth location. As previously noted, there was a high degree of difficulty involved with constructing a mesh with consistent element geometry at this

location. Therefore, the elements forming the mesh construction may not accurately represent the stress distributions and model parameters and this directly impacted the stress intensity value solution.

In a scenario where the mesh may not properly depict the stress distribution, a partial safety factor would typically be applied to the stress component calculation. For the model in this evaluation, the partial safety factor would be characterized by a coefficient of variation (COV_s); the COV_s is classified as the ratio of the standard deviation of the distribution to the mean of the distribution. The appropriate COV_s accounts for the uncertainty in the model estimates of the stress. Since the computed stresses in this model are "reasonably well known," further uncertainty would warrant a greater COV_s [16]. Therefore, the application of a COV_s adds a minimum partial safety factor of 1.40 to the calculated stress. The partial safety factor could reach as high as 4.10 depending on the probability of failure, safety index, and regions of plastic collapse parameters. Part 9 of the API 579-1/ASME FFS-1 standard [16] contains the calculations for the necessary COV_s.

The magnitude of the partial safety factor warranted by the standard at the surface location outweighs the degree of conservatism found at the depth location. The crack construction in this research did not produce reliable stress intensity solutions at the surface location of the contour. As a result, this research could not evaluate the level of conservatism at the surface location of a semi-elliptical flaw through the use of this model construction.

5.2 Summary

The API 579-1/ASME FFS-1 standard returned conservative solutions at the depth location that were equivalent to incorporating a safety factor of 1.375 and 1.385 for Load 1 and

Load 2 respectively. The difficulties in constructing a consistent mesh geometry at the surface location called for the application of additional safety factors. This obstacle interfered with the reliability of the stress intensity calculations. Overall, this specific model construction did not permit the appropriate characterization of the level of conservatism at the surface location of the semielliptical crack contour.

Chapter 6

Conclusions

A better understanding of failure phenomena leads to improved structural reliability and confidence in strength predictions. This research was the first step in further understanding the conservatism contained in the critical crack-like flaw assessment in the API 579-1/ASME FFS-1standard. The construction of a flat plate model containing a semi-elliptical crack was used to analyze this standard through comparative methods. The critical crack-like assessment is directly dependent on the comparison between stress intensity factors and the material fracture toughness. Standard parameters were used for the construction of the model, and a load with two different magnitudes was applied through the thickness of the plate. This load was characterized by a high stresses that decreased rapidly moving away from the surface

The API 579-1/ASME FFS-1 standard only allows for the evaluation of stress intensity factors at the depth and surface locations on the semi-elliptical crack contour; therefore, these were the two solutions used for comparison. Evaluation of the depth, or 90 degree location showed that the standard is indeed conservative when calculating critical crack values. The API 579-1/ASME FFS-1 standard was found to have additional 1.375 and 1.385 safety factors built into the assessment; this was determined through the comparison to the ABAQUS/CAE model. Additionally, the solutions from Niu and Glinka's weight function method for surface semi-elliptical cracks for plates with a finite thickness were compared to those given by the standard. This comparison was also used to check the validity of the weight function results provided by the standard.

The surface, or zero degree, location of the API 579-1/ASME FFS-1 standard gave stress intensity results similar to those provided by the ABAQUS/CAE model. These surface results did not display the same level of conservatism as the depth location results; difficulties in constructing the mesh at the surface location may account for this disagreement. In this situation, a minimum partial factor of safety of 1.40 would need to be applied to this value. Consequently, the level of conservatism at the surface location was unable to be assessed due to the geometric inconsistencies in the model.

Chapter 7

Future Work

Further research must be performed to both reinforce the findings for the depth and to assess the stress intensity at the surface locations of a semi-elliptical flaw. The goal is for this research to supply a better understanding of the conservatism of the critical crack assessment. This knowledge can ultimately help balance the seesaw between business endeavors and structural integrity of the equipment in the refinery and petrochemical industry.

The first application is further inspection of the two locations of the semielliptical flaw. The findings at the depth location should be reinforced; in addition, the degree of conservatism at the surface location must be evaluated. The second task for future work is to evaluate a bivariant loading case varying along the surface of the crack as well as the depth. The ultimate goal is to construct a bivariant weight function accurately characterizing a surface semi-elliptical crack. This can lead to accurate critical crack-like flaw assessments when the flaw is exposed to high surface residual stress profiles.

7.1 Modeling Work

One important aspect of the future modeling work is to design a consistent mesh at the surface location. This construction may be achieved by involving a different crack contour and/or manipulating partitions. The wedge elements need to accurately reflect the applied stresses so the level of conservatism can be approximated. A second task is to construct several semi-elliptical crack contours with varying dimensions and observe whether the conservative results vary with

crack geometry. In addition, another modeling task is to apply varying load profiles to these models and evaluate the degree of variance in the solutions. As stated, the next stage in this research is to analyze the stress intensity profile along the surface of the crack; thus, the newly constructed models would be utilized in this application as well.

7.2 Analytical Work

The future analytical work stems directly from the modeling work. Solutions obtained from the modeling work need to be compared to the API 579-1/ASME FFS-1 critical crack-like flaw assessment via Mathcad; the stress profiles would need to be fit to polynomials for this analysis as well. The final key application in this area will be the construction of a bivariant weight function for the through-thickness and surface profiles.

References

[1] R. Laggoune, A. Chateauneuf, D. Aissani, "Opportunistic policy for optimal preventive maintenance of a multi-component system in continuous operating units," *Computers and Chemical Engineering,* Vol. 33, pp 1499-1510, 2009.

[2] "We do more than inspections: TÜV Rheinland Partnering the chemical industry," *Compendium Industrial Park, Chemical and Pharmaceutical Industry, Biotech*, pp. 50, 2008.

[3] S. Chattopadhyay, Pressure Vessels: Design and Practice. CRC Press LLC, Florida, 2005.

[4] J.S. Hornsey, "Residual Stresses: Their causes, and the Effective Means of Treatment to Reduce the Residual Stresses and to Improve the Fatigue Life in Engineering Components," January 2006. Available online http://www.wibropol.eu/uploads/literatura/Residual%20Stresses.pdf.

[5] R. Ainsworth, J. Sharples, and S. Smith, "Effects of Residual Stresses on Fracture Behavior-experimental results and assessment methods," *Journal of Strain Analysis,* Vol. 35, No. 4, pp. 307-316, 2000.

[6] P. Dong, J. Hong, "Recommendations for determining residual stresses in fitness-for-service assessment," *Welding Research Council,* Bulletin 476, November 2002.

[7] S. Lewis, C. Truman, D. Smith, "A comparison of 2D and 3D fracture assessments in the presence of residual stresses," *2007 ASME Pressure Vessels and Piping Division Conference.* San Antonio, Texas, 22-26 July, 2007.

[8] P.M. Besuner, "The influence function method for fracture mechanics and residual fatigue life analysis of cracked components under complex stress fields," *Nuclear Engineering and Design,* Vol. 43, pp. 115-154, 1976.

[9] "Fracture Toughness," *NDT Education Resource Center, Brian Larson, Editor,* 2001-2010, The Collaboration for NDT Education, Iowa State University. Available online www.ndt-ed.org.

[10] X. B. Lin, R. A. Smith, "Fatigue growth prediction of internal surface cracks in pressure vessels," *Journal of Pressure Vessel Technology-Transactions of the ASME,* Vol. 120, pp.17-23, 1998.

[11] H. Khoramishad, M. R. Ayatollahi, "Finite element analysis of a semi-elliptical external crack in a buried pipe," *Fatigue and Fracture Lab, Department of Mechanical Engineering, Iran University of Science and Technology,* August 2009.

[12] "Annex C," API. Recommended practice for fitness-for-service. API 579. Washington, DC: American Petroleum Institute, 2007.

[13] T. Anderson, D. Osage, "API 579: a comprehensive fitness-for-service guide," *International journal of Pressure Vessels and Piping,* Vol. 77, pp. 953-963, 2000.

[14] "Process equipment fitness for service assessments using API RB 579," *Technical Software Services Limited,* 2009. Available online http://www.tech-soft.co.uk/fit_service_01.html.

[15] "Front Matter," API. Recommended practice for fitness-for-service. API 579. Washington, DC: American Petroleum Institute, 2007.

[16] "Section 9," API. Recommended practice for fitness-for-service. API 579. Washington, DC: American Petroleum Institute, 2007.

[17] "Annex D," API. Recommended practice for fitness-for-service. API 579. Washington, DC: American Petroleum Institute, 2007.

[18] D. Lee, C. McClung, G. Chell, "An efficient stress intensity factor solution scheme for corner cracks at holes under bivariant stressing," *Fatigue and Fracture of Engineering Materials and Structures.* Southwest Research Institute, San Antonio, Texas, 2008.

[19] X. Niu, G. Glinka, "Weight Functions for edge and surface semi-elliptical cracks in flat plates and plates with corners," *Engineering Fracture Mechanics.* Vol. 36, No. 3, pp 459-475, 1990.

[20] J. C. Newman and I. S. Raju, Stress intensity factors equations for cracks in three dimensional finite bodies subjected to tension and bending loads, in *Computational Methods in the Mechanics of Fracture,* pp. 311-334, North Holland, Amsterdam (1986).

[21] C. Leondes, Structural Dynamic Systems Computational Techniques and Optimization: Finite Element Analysis Techniques. Gordon and Breach Science Publishers: Amsterdam, 1998.

[22] Jinsan Ju, "Calculation and Comparison of Fracture Parameter of 3-D Thin-Walled Structure in ANSYS," Department of Civil Engineering, National University of Ireland, Galwy

Appendix A

Overview of the Assessment Procedure: Critical Crack-like Flaw Assessment [16]

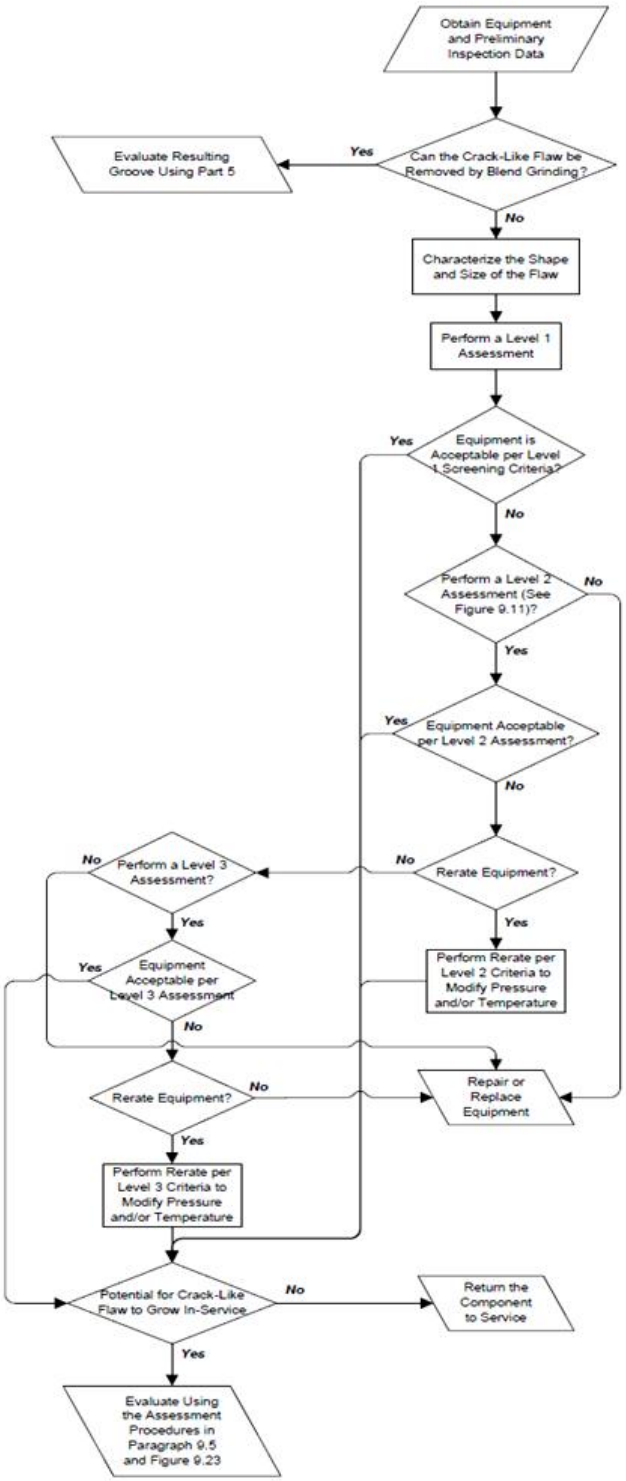

Appendix B

Stress Distributions: Stress Through-thickness for Load 1

x	S11	S22	S33	S12	S13	S23
0	0.0460798	54.4229	44198.1	-1.67775	-0.0006505	0.0202145
0.0300059	0.067442	54.7136	44173.1	-2.24629	-0.00075	0.0201325
0.0600117	0.109604	54.9847	43842.9	-3.3177	-0.0010576	0.0199974
0.0900176	0.149943	55.1968	42967.3	-4.3398	-0.0013605	0.0198512
0.120023	0.187339	55.3528	41553.7	-5.28765	-0.0016371	0.0196972
0.150029	0.221877	55.4576	39635.3	-6.16134	-0.0018953	0.0195378
0.180035	0.253559	55.5161	37259	-6.96107	-0.0021296	0.019374
0.210041	0.282353	55.5331	34484.1	-7.68702	-0.0023436	0.0192068
0.240047	0.308241	55.5135	31380.5	-8.33938	-0.0025353	0.0190364
0.270053	0.331257	55.4623	28026.8	-8.91838	-0.0027057	0.0188633
0.300059	0.351413	55.3843	24507.4	-9.42421	-0.0028547	0.0186881
0.330065	0.368692	55.2842	20910.3	-9.85713	-0.0029819	0.0185116
0.36007	0.383096	55.167	17324	-10.2174	-0.0030878	0.0183345
0.390076	0.394617	55.0374	13834.8	-10.5052	-0.0031728	0.0181574
0.420082	0.403237	54.9003	10524.4	-10.7208	-0.0032356	0.0179812
0.450088	0.408987	54.7605	7466.84	-10.8646	-0.0032775	0.0178066
0.480094	0.411893	54.6227	4726.54	-10.9367	-0.0032979	0.017634
0.5101	0.411965	54.4915	2356.35	-10.9375	-0.0032978	0.0174647
0.540106	0.409224	54.3773	395.88	-10.8696	-0.0032754	0.0172966
0.570111	0.403787	54.2832	-1129.49	-10.7328	-0.0032337	0.0171321
0.600117	0.395491	54.2092	-2209.25	-10.5253	-0.0031684	0.0169716
0.630123	0.384405	54.1599	-2847.82	-10.2473	-0.0030842	0.0168173
0.660129	0.370482	54.1401	-3064.1	-9.89914	-0.0029776	0.0166688
0.690135	0.353799	54.1545	-2890.53	-9.48101	-0.0028502	0.0165276
0.720141	0.334328	54.2078	-2371.66	-8.9932	-0.0027015	0.0163936
0.750147	0.31212	54.3045	-1562.32	-8.43598	-0.0025319	0.016268
0.780153	0.287075	54.4517	-518.744	-7.80697	-0.0023406	0.0161518
0.810158	0.259319	54.6521	677.499	-7.10921	-0.0021282	0.0160452
0.840164	0.228882	54.9101	1955.16	-6.343	-0.0018951	0.0159491
0.87017	0.195761	55.2304	3243.47	-5.50863	-0.001641	0.0158638
0.900176	0.159981	55.6174	4474.93	-4.60644	-0.0013664	0.0157905
0.930182	0.121548	56.0757	5587.95	-3.63671	-0.001071	0.0157293
0.960188	0.0804487	56.6099	6529.33	-2.59982	-0.000755	0.0156815
1.0002	0.0456229	57.208	7198.87	-1.72595	-0.0004837	0.0156543

Stress Distributions: Stress Through-thickness for Load 2

x	S11	S22	S33	S12	S13	S23
0	0.0869452	11.2251	35873.4	-0.998893	-0.462649	5.0769
0.0250714	0.105479	11.3068	35856.9	-1.12094	-0.528844	5.14294
0.0501429	0.136794	11.441	35679.1	-1.32728	-0.640962	5.25752
0.0752143	0.171376	11.5816	35251	-1.55241	-0.763878	5.38709
0.100286	0.204411	11.7058	34531.6	-1.76365	-0.880069	5.51496
0.125357	0.235779	11.8145	33528.1	-1.96115	-0.989614	5.64126
0.150429	0.264991	11.9045	32171.2	-2.14086	-1.09034	5.7658
0.1755	0.292489	11.9817	30576.3	-2.30745	-1.18459	5.88923
0.200571	0.318248	12.0471	28766.3	-2.46114	-1.27237	6.01171
0.225643	0.342239	12.1016	26765.8	-2.6021	-1.35374	6.13338
0.250714	0.364427	12.146	24601.7	-2.73046	-1.42879	6.2544
0.275786	0.384114	12.1787	22278.9	-2.84236	-1.49545	6.37485
0.300857	0.401905	12.2039	19885.1	-2.94209	-1.55594	6.4951
0.325929	0.417743	12.2226	17452.8	-3.02979	-1.6103	6.6153
0.351	0.431601	12.2354	15014.9	-3.10557	-1.65856	6.73559
0.376071	0.443482	12.2432	12604	-3.16955	-1.70081	6.85614
0.401143	0.452617	12.2461	10291.8	-3.21798	-1.7351	6.97732
0.426214	0.459723	12.2463	8096.81	-3.25493	-1.76352	7.0992
0.451286	0.464754	12.2447	6044.73	-3.28046	-1.7861	7.22194
0.476357	0.467704	12.2421	4158.92	-3.29466	-1.8029	7.34568
0.501429	0.468604	12.2391	2460.69	-3.29765	-1.81396	7.47058
0.5265	0.466706	12.2372	1045.3	-3.28581	-1.81744	7.59732
0.551571	0.462778	12.237	-141.57	-3.26302	-1.81532	7.72568
0.576643	0.456802	12.2394	-1094.71	-3.22934	-1.80761	7.8558
0.601714	0.448796	12.2449	-1811.81	-3.18486	-1.79436	7.98784
0.626786	0.438818	12.2542	-2293.49	-3.12968	-1.7756	8.12195
0.651857	0.426205	12.2699	-2473.79	-3.06039	-1.74955	8.2591
0.676928	0.411721	12.2914	-2445.37	-2.98069	-1.71808	8.39878
0.702	0.395383	12.3192	-2224.5	-2.89066	-1.68121	8.54111
0.727071	0.37724	12.3539	-1829.46	-2.79041	-1.63896	8.68626
0.752143	0.357371	12.3962	-1280.48	-2.68007	-1.59134	8.83436
0.777214	0.335273	12.4496	-572.882	-2.55646	-1.5366	8.98668
0.802285	0.311642	12.5122	215.632	-2.42314	-1.47652	9.14238
0.827357	0.286538	12.5846	1058.75	-2.28022	-1.4111	9.3016
0.852428	0.26004	12.6672	1930.25	-2.12785	-1.34036	9.46446
0.8775	0.232251	12.7607	2804.01	-1.9662	-1.26428	9.6311
0.902571	0.202912	12.8696	3631.16	-1.7925	-1.18107	9.80304
0.927642	0.172564	12.9908	4389.73	-1.61006	-1.09249	9.97912
0.952714	0.141326	13.1249	5060.68	-1.41908	-0.998528	10.1595
0.977785	0.113463	13.251	5581.93	-1.24636	-0.912716	10.3202
1.00286	0.0973863	13.327	5848.37	-1.14534	-0.862143	10.4133

Appendix C

Weight Function Calculations: API 579-1/ASME FFS-1 Mathcad Assessment

$$a := 0.2 \qquad c := 1.42266 \qquad t := 1.0 \qquad W := 5.0$$

$$Q := \begin{cases} \left[1.0 + 1.464\left(\frac{c}{a}\right)^{1.65}\right] & \text{if } \left(\frac{a}{c}\right) > 1.0 \\ \left[1.0 + 1.464\left(\frac{a}{c}\right)^{1.65}\right] & \text{otherwise} \end{cases}$$

$$A_0 := 0.456128 - 0.114206\left(\frac{a}{c}\right) - 0.046523\left(\frac{a}{c}\right)^2$$

$$A_1 := 3.022 - 10.8679\left(\frac{a}{c}\right) + 14.94\left(\frac{a}{c}\right)^2 - 6.8537\left(\frac{a}{c}\right)^3$$

$$A_2 := -2.28655 + 7.88771\left(\frac{a}{c}\right) - 11.0675\left(\frac{a}{c}\right)^2 + 5.16354\left(\frac{a}{c}\right)^3$$

$$B_0 := 1.10190 - 0.019863\left(\frac{a}{c}\right) - 0.043588\left(\frac{a}{c}\right)^2$$

$$B_1 := 4.32489 - 14.9372\left(\frac{a}{c}\right) + 19.4389\left(\frac{a}{c}\right)^2 - 8.52318\left(\frac{a}{c}\right)^3$$

$$B_2 := -3.03329 + 9.96083\left(\frac{a}{c}\right) - 12.582\left(\frac{a}{c}\right)^2 + 5.52318\left(\frac{a}{c}\right)^3$$

$$Y_0 := B_0 + B_1 \cdot \left(\frac{a}{t}\right)^2 + B_2 \cdot \left(\frac{a}{t}\right)^4 \qquad Y_1 := A_0 + A_1 \cdot \left(\frac{a}{t}\right)^2 + A_2 \cdot \left(\frac{a}{t}\right)^4$$

$$M_1 := \frac{\pi}{\sqrt{2 \cdot Q}} \cdot \left(4 \cdot Y_0 - 6 \cdot Y_1\right) - \frac{24}{5}$$

$$M_2 := 3$$

$$M_3 := 2 \cdot \left(\frac{\pi}{\sqrt{2 \cdot Q}} \cdot Y_0 - M_1 - 4\right)$$

$$h_{90} := \frac{2}{\sqrt{2\cdot\pi\cdot(a-x)}}\cdot\left[1 + M_1\cdot\left(1-\frac{x}{a}\right)^{\frac{1}{2}} + M_2\cdot\left(1-\frac{x}{a}\right) + M_3\cdot\left(1-\frac{x}{a}\right)^{\frac{3}{2}}\right]$$

$$\delta := 0.448863 - 0.173295\left(\frac{a}{t}\right) - 0.267775\left(\frac{a}{t}\right)^2 \qquad \gamma := 0.976770 - 0.131975\left(\frac{a}{t}\right) - 0.484875\left(\frac{a}{t}\right)^2$$

$$\alpha := 1.14326 + 0.0175996\left(\frac{a}{t}\right) + 0.501001\left(\frac{a}{t}\right)^2 \qquad \beta := 0.458320 - 0.102985\left(\frac{a}{t}\right) - 0.398175\left(\frac{a}{t}\right)^2$$

$$F_1 := \gamma\cdot\left(\frac{a}{c}\right)^{\delta} \qquad F_0 := \alpha\cdot\left(\frac{a}{c}\right)^{\beta}$$

$$N_1 := \frac{\pi}{\sqrt{4\cdot Q}}\cdot\left(30\cdot F_1 - 18\cdot F_0\right) - 8 \qquad N_2 := \frac{\pi}{\sqrt{4\cdot Q}}\cdot\left(60\cdot F_0 - 90\cdot F_1\right) + 15 \qquad N_3 := -\left(1 + N_1 + N_2\right)$$

$$h_0 := \frac{2}{\sqrt{\pi\cdot x}}\cdot\left[1 + N_1\cdot\left(\frac{x}{a}\right)^{\frac{1}{2}} + N_2\cdot\left(\frac{x}{a}\right) + N_3\cdot\left(\frac{x}{a}\right)^{\frac{3}{2}}\right]$$

$$f_W := \left(\sec\left(\sqrt{\frac{a}{t}}\cdot\frac{\pi\cdot c}{2\cdot W}\right)\right)^{0.5}$$

$$K_{90} := \left[\int_0^a \left|(\sigma(x,a))\cdot\left(h_{90}\right)\right| dx\right]\cdot f_W \qquad K_0 := \left[\int_0^a \left|(\sigma(x,a))\cdot\left(h_0\right)\right| dx\right]\cdot f_W$$

Weight Function Calculations: Niu and Glinka Mathcad Assessment

$$a := 0.2 \qquad c := 1.42266 \qquad t := 1.0 \qquad w := 10.0 \qquad \phi := (0, 90)$$

$$Q := 1 + 1.464\left(\frac{a}{c}\right)^{1.65} \qquad \gamma := \left[\frac{(\pi \cdot c)}{w}\right] \cdot \sqrt{\frac{a}{t}}$$

$$h := \sqrt{\sec(\gamma)} \qquad f := \left[\left(\frac{a}{c}\right)^2 \cdot (\cos(\phi))^2 + (\sin(\phi))^2\right]^{\left(\frac{1}{4}\right)} \qquad g := 1 + \left[0.1 + 0.35\left(\frac{a}{t}\right)^2\right] \cdot (1 - \sin(\phi))^2$$

$$A_1 := 1.13 - 0.09\left(\frac{a}{c}\right) \qquad A_2 := -0.54 + \frac{0.89}{\left(0.2 + \frac{a}{c}\right)} \qquad A_3 := 0.5 - \left[\frac{1}{\left(0.65 + \frac{a}{c}\right)}\right] + 14\left(1 - \frac{a}{c}\right)^{24}$$

$$F := \left[A_1 + A_2\left(\frac{a}{t}\right)^2 + A_3\left(\frac{a}{t}\right)^4\right] \cdot \frac{(g \cdot f \cdot h)}{\sqrt{Q}}$$

$$E_0 := 1 \qquad E_2 := -1 \qquad E_4 := 5 \qquad E_6 := -6 \qquad E_8 := 1358 \qquad E_{10} := -5052 \qquad E_{12} := 2702765$$

$$E_{14} := -199360981 \qquad E_{16} := 19391512145 \qquad E_{18} := -2404879675441 \qquad E_{20} := 370371188237525$$

$$C_1 := (A_1)^2 \qquad C_2 := 2 \cdot A_1 \cdot A_2 \qquad C_3 := (A_2)^2 + 2 \cdot A_1 \cdot A_3 \qquad C_4 := 2 \cdot A_2 \cdot A_3 \qquad C_5 := (A_3)^2$$

$$A := 0.5\left[\frac{(\pi \cdot c)}{w}\right] \cdot \sqrt{\frac{a}{t}} \cdot t \cdot g \cdot \left[\sqrt{\frac{a}{t}} \cdot \frac{(\pi\, c)}{w}\right] + 4\left[\frac{\left[A_2\left(\frac{a}{t}\right)^2 + 2A_3\left(\frac{a}{t}\right)^4\right]}{\left[A_1 + A_2\left(\frac{a}{t}\right)^2 + A_3\left(\frac{a}{t}\right)^4\right]}\right]$$

$$B := \sum_{n=10}^{10} \sum_{p=1}^{5} \left[\left[\left[\frac{\left(\frac{\pi\, c}{w}\right)^{(2n)} (-1)^n E_{(2n)}}{(2n)!}\right] \cdot \frac{(C_p)}{(2p + n)}\right] \cdot \left(\frac{a}{t}\right)^{(2p+n-2)} \cdot \left[\frac{\left(5\sqrt{2\pi}\right)}{8Q \cdot F}\right]\right]$$

$$M_1 := A + 3B - 4 \qquad M_2 := 5\cdot\left[\left[\frac{\left(\sqrt{2}\pi\right)}{4}\right]F - \left[\frac{(A-1)}{3}\right] - B\right]$$

$$m := \left[\frac{2}{\left[\sqrt{2\pi(a-x)}\right]}\right]\cdot\left[1 + M_1\left[\frac{(a-x)}{a}\right] + M_2\left[\frac{(a-x)}{a}\right]^2\right]$$

$$K := \int_0^{0.2}\left[(\text{Stress})\cdot\left[\left[\frac{2}{\left[\sqrt{2\pi(a-x)}\right]}\right]\cdot\left[1 + M_1\left[\frac{(a-x)}{a}\right] + M_2\left[\frac{(a-x)}{a}\right]^2\right]\right]\right] dx$$

ACADEMIC VITA OF KATELYN SMITH

Name: Katelyn J. Smith

E-mail ID: KJS5094

Address: 160 Argyle Rd, Langhorne PA, 19047

Education Major: Engineering Science
Education Minor: Engineering Mechanics
Honors: Engineering Science and Mechanics

Thesis Title: Evaluation of the Criteria for Crack Propagation in the Presence of High Surface Stresses
Thesis Supervisor: Dr. A. Segall

Work Experience:

May 2009 - August 2009
Mechanical Engineer, Intern
Fitness-For-Service Section
The Equity Engineering Group in Shaker Heights, Ohio

Grants Received:
The Pennsylvania State University Bookstore Scholarship, Leonhard Honors Program

Awards:
Dean's List (Fall 2006, Spring 2007, Spring 2008, Spring 2009, Fall 2009), Rotary Club Commended Scholar, Integrated Undergraduate Graduate Program

Memberships:
The Pennsylvania University's Women in Engineering Program, William and Wyllis Leonhard Scholars Program, The Pennsylvania Epsilon Chapter of Pi Beta Phi, Society of Engineering Science

Community Service Involvement:
The Pennsylvania State University Dance Marathon, We are Curing Autism Now 5K Run/ 3K Walk, Read Across America Day, Champions are Readers, Volunteer at the Princeton Medical Center